Structures of Three Inhibitor Complexes Provide Insight into the Reaction Mechanism of the Human Methylenetetrahydrofolate Dehydrogenase/ Cyclohydrolase

Andrea Schmidt,[‡] Haiping Wu,[§] Robert E. MacKenzie,[§] Victor J. Chen,[||] Jesse R. Bewly,[||] James E. Ray,[||] John E. Toth,[||] and Miroslaw Cygler*,[‡]

Biotechnology Research Institute, National Research Council of Canada, Montreal Joint Centre for Structural Biology, 6100 Royalmount Avenue, Montreal, Quebec H4P 2R2 Canada, Faculty of Medicine, McGill University, 845 Sherbrooke Street, Montreal, Quebec H3A 2T5 Canada, and Lilly Research Laboratories, Indianapolis, Indiana 46285

Received November 29, 1999; Revised Manuscript Received March 7, 2000

ABSTRACT: Enzymes involved in tetrahydrofolate metabolism are of particular pharmaceutical interest, as their function is crucial for amino acid and DNA biosynthesis. The crystal structure of the human cytosolic methylenetetrahydrofolate dehydrogenase/cyclohydrolase (DC301) domain of a trifunctional enzyme has been determined previously with a bound NADP cofactor. While the substrate binding site was identified to be localized in a deep and rather hydrophobic cleft at the interface between two protein domains, the unambiguous assignment of catalytic residues was not possible. We succeeded in determining the crystal structures of three ternary DC301/NADP/inhibitor complexes. Investigation of these structures followed by site-directed mutagenesis studies allowed identification of the amino acids involved in catalysis by both enzyme activities. The inhibitors bind close to Lys56 and Tyr52, residues of a strictly conserved motif for active sites in dehydrogenases. While Lys56 is in a good position for chemical interaction with the substrate analogue, Tyr52 was found stacking against the inhibitors' aromatic rings and hence seems to be more important for proper positioning of the ligand than for catalysis. Also, Ser49 and/or Cys147 were found to possibly act as an activator for water in the cyclohydrolase step. These and the other residues (Gln100 and Asp125), with which contacts are made, are strictly conserved in THF dehydrogenases. On the basis of structural and mutagenesis data, we propose a reaction mechanism for both activities, the dehydrogenase and the cyclohydrolase.

Tetrahydrofolate (THF)[1] plays a crucial role as a molecule for the production and utilization of monocarbon units in various oxidation states. THF derivatives participate in a variety of biosyntheses, including methionine, glycine, serine, purine bases, and thymidylate (*1*). Therefore, it is not surprising that several enzymes exist to link and subsequently modify these one-carbon units on the THF molecules. These enzymes play a vital role for the production and also the degradation of some amino acids and nucleotides, as well as the maintenance of the required levels of methyl-, methylene-, formyl- and unsubstituted THF.

In higher organisms, the activities involved in the modification of the monocarbon that can be transferred as a methylene, methenyl, or formyl group are linked together to form a trifunctional enzyme consisting of methylene-THF dehydrogenase (D), methenyl-THF cyclohydrolase (C), and 10-formyl-THF synthetase (S) (*2*). Therefore, these enzymes represent potential pharmaceutical targets for the manipulation of cell growth and development and hence cancer prevention or treatment.

The crystal structure of DC301, the human cytosolic DC domain of the trifunctional enzyme, has been determined previously to 1.5 Å resolution (*3*), and the structure of the *Escherichia coli* enzyme was published recently (*4*). DC301 was cocrystallized with NADP, which is used as a cofactor in the dehydrogenase step. NADP binds to the C-terminal domain, which shows the typical Rossmann fold (*5*) observed in the SCAD protein family (*6*). The position of the cofactor's nicotinamide ring in a large, rather hydrophobic cleft and in the vicinity of the Y−X−X−X−K motif strictly conserved in this family (*6*, *7*) indicated the likely location of the active site. Nevertheless, an unambiguous assignment of the roles of residues involved in catalysis could not be made.

Various structures of dehydrogenase complexes with either NAD or NADP cofactors have been determined (*8*−*12*), and some of them have also been cocrystallized with a substrate analogue (*13*−*15*). However, no information on the enzyme−cofactor complex exists for the family represented by human bifunctional DC301 enzyme. The details of the reaction mechanism, which includes channeling (*16*) between the two catalytic activities (D and C, Figure 1), remain to be determined.

* Corresponding author. Telephone: (514)496 6321. Fax: (514)-496 5143. E-mail: mirek.cygler@bri.nrc.ca.

[‡] National Research Council of Canada.

[§] McGill University.

[||] Lilly Research Laboratories.

[1] Abbreviations: THF, tetrahydrofolate; DC, dehydrogenase/cyclohydrolase; calcd, calculated; NADP, nicotinamide adenine dinucleotide phosphate; MOPS, 3-(*N*-morpholino)propanesulfonic acid; SCAD, short-chain alcohol dehydrogenase; PEG, poly(ethylene glycol); DMSO, dimethyl sulfoxide; PMSF, phenylmethanesulfonyl fluoride; BSA, bovine serum albumin.

10.1021/bi992734y CCC: $19.00
Published on Web 05/02/2000

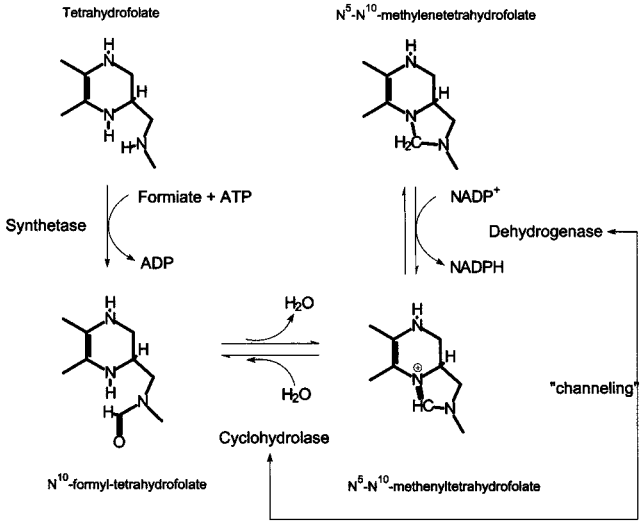

FIGURE 1: Pathways in THF metabolism showing the function of the methylene-THF dehydrogenase (D), cyclohydrolase (C) DC301, and 10-formyl-THF synthetase, the third activity of the full-length protein DCS. Only the reactive part of the THF molecule is shown.

To elucidate the reaction mechanisms for each of the two enzymatic activities, we undertook crystallographic studies of ternary complexes of DC301, NADP, and several folate analogue inhibitors, some of which are already in clinical trials (*17*−*19*). Three of the inhibitors were successfully cocrystallized with the enzyme and NADP. These crystal structures provided insight that allowed us not only to identify the catalytic residues but also to propose a plausible reaction mechanism for both reaction steps.

EXPERIMENTAL PROCEDURES

Crystallization of Protein−*Inhibitor Complexes.* The protein DC301 was kept in a solution containing 50 mM potassium phosphate buffer at pH 7.3, 1 mM benzamidine, 20% glycerol, 35 mM β-mercaptoethanol, and 7 mM NADP at a concentration of 12−20 mg/mL. This solution was diluted 1:1 with 10 mM potassium phosphate buffer, pH 6.8, prior to crystallization, and 1 μL of β-mercaptoethanol was added per 250 μL of final solution.

The inhibitors used in this study were provided by Eli Lilly and are shown in Figure 2. Complexes with inhibitors were obtained by cocrystallization at different protein/inhibitor ratios. The compounds Ly345899, Ly249543, Ly374571, and Ly289739 (molecular mass between 423 and 471 g/mol) as shown in Figure 2 (*17*−*19*) were solids and were dissolved in 10 mM KH_2PO_4, pH 6.8, containing 1 μL of β-mercaptoethanol/125 μL. This solution was then used as a diluent for the protein to give approximate protein/inhibitor ratios of 1:100 for Ly249543 and Ly289739 or 1:10 for Ly345899 and Ly374571.

Crystals were obtained by hanging drop vapor diffusion at 20 °C at conditions similar to that of the native enzyme (*20*). The precipitant contained 25% (w/v) PEG 3350, 0.2 M ammonium acetate, 5% glycerol, and 0.1 M sodium citrate, pH 5.2. Drops contained 2 μL of protein solution and 4 μL of reservoir solution. Native crystals were used as the initial macroseeds. This process initiated nucleation, and the new crystals were transferred into new inhibitor-containing drops for their final growth. When the inhibitors are present, the crystals grow to smaller size than native

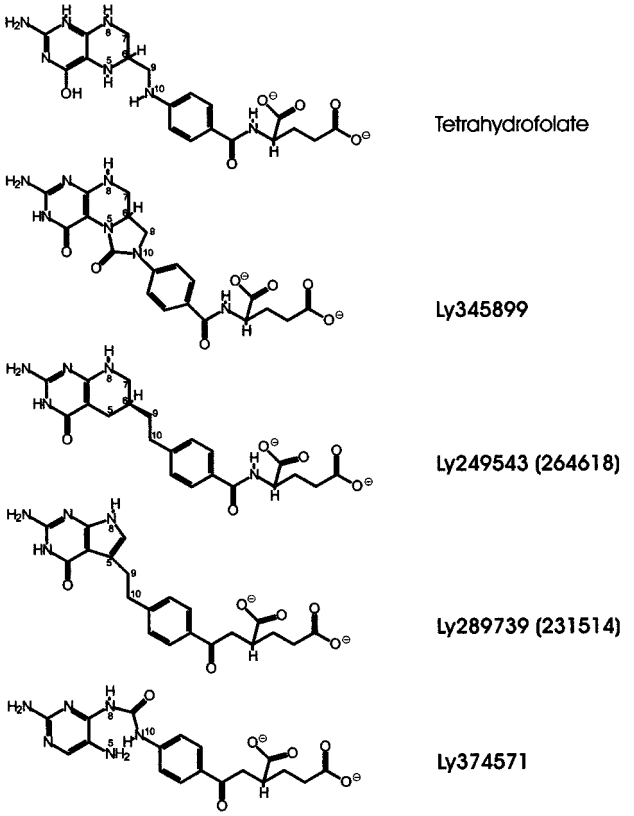

FIGURE 2: Four inhibitors used are shown with THF as a reference. Atoms belonging to the reactive part are numbered. Inhibitor Ly289739 did not bind to DC301 under our crystallization conditions despite its low K_i. Figure drawn with ChemWindows, version 5.0 (SoftShell Int. Ltd.).

crystals and appear to be more fragile. For data collection, the crystals were mounted in a nylon fiber loop and shock frozen in liquid nitrogen or in the cold stream of nitrogen gas (Oxford Cryosystem, set at 100 K) either immediately or after a brief soak in heavy mineral oil.

Data Collection and Processing. Data collection for complexes with Ly249543, Ly289739, and Ly374571 was carried out at 100 K on a Quantum-4 CCD detector at the beamline X8C, NSLS, BNL, Upton, NY. The wavelength was 1.00022 Å, the crystal to detector distance was 175 mm, and the oscillation range was 0.75° per frame with exposure times of 30−50 s. Dezingering was applied for longer exposure times. Data for the Ly345899 complex were collected with an oscillation range of 1.5° and a crystal-to-detector distance of 140 mm on an RAXIS-II C detector mounted on a RU-300 rotating anode generator. Data reduction was carried out with programs DENZO and SCALEPACK (*22*), and reflection files were converted into CNS format with the program "sca2cns" of the CCP4 package (*23*).

Crystals of DC301 complexes form platelets with dimensions 0.3 × 0.3 × 0.05 mm and belong to the space group $P2_12_12_1$ with cell constants $a = 67.7$, $b = 135.9$, $c = 61.6$ Å and two molecules in the asymmetric unit. The complexes diffracted to a maximum resolution of 2.1−2.2 Å as compared to the native crystals that diffracted to a resolution of 1.5 Å. A summary of the statistics for the datasets used for structure refinement is given in Table 1.

Structure Refinement. Refinement was carried out with CNS version 0.5 (*24*). The native protein structure without

Table 1: Data Collection Statistics for the Datasets Collected on the Inhibitor Complexes[a]

inhibitor	reflections total	reflections unique	resolution (Å)	R_{sym}	$I/\sigma(I)$	completeness (%)	redundancy
Ly345899	185 463	15 688	20.0−2.7	10.0	≥4	97.1	6
Ly249543	175 474	29 512	15.0−2.2	4.4	≥4	99.3	4
Ly374571	238 477	29 628	15.0−2.2	4.4	>5	99.8	5
Ly289739	256 517	33 662	15.0−2.1	4.9	>5	99.0	4−5

[a] In all cases except Ly289739, the inhibitor was actually bound.

Table 2: Refinement Statistics for the Three Complexes[a]

		Ly345899	Ly249543	Ly374571
resolution range (Å)		8−2.7	15−2.2	15−2.2
no. of reflections (total)		15 194	28 962	26 225
no. of atoms (total, non-H)		4638	4722	4753
of which	protein (A + B)	4391	4398	4398
	water	110	195	218
	NADP (A + B)	96	96	96
	inhibitor	34	32	31
	other heteroatoms			4
individual B factors refined		no	yes	yes
bulk solvent correction		yes	yes	yes
average B factor overall		not refined	24.6	24.5
of which	protein	not refined	24.2	23.6
	water	not refined	28.2	29.0
	NADP	not refined	41.0	50.7
	inhibitor	not refined	11.3	24.3
	other heteroatoms			47.3
R		20.7	22.7	22.6
R_{free} (10% of data)		23.1	26.4	26.7

[a] In the refinement process, no noncrystallographic restraints or σ cutoffs on the data were applied.

NADP or water was used as the starting model for rigid body refinement. The resolution ranges were 15−2.2 Å for inhibitors Ly249543 and Ly374571 and 8−2.7 Å for inhibitor Ly345899. All reflections were included in the refinement. To monitor the progress of the refinement, 10% of the data were set aside for cross-validation using R_{free} (*25*).

After rigid body refinement and a first round of positional refinement, two NADP molecules and several water molecules were inserted manually into the electron density ($2F_o-F_c$ and F_o-F_c maps) using version 6.2.1 of the program O (*26*). After several rounds of refinement, adding more solvent molecules and applying bulk solvent correction, electron density near one of the molecules of the noncrystallographic dimer was sufficiently clear to add the inhibitor (with the exception of Ly289739; no inhibitor was found). There was no evidence for the presence of an inhibitor in the second molecule. In all cases except Ly345899, in which the resolution was insufficient, individual B factors were refined. Because of the structural differences between the two monomers, noncrystallographic symmetry restraints were not applied. Topology and parameter files for the inhibitors and NADP were setup using the existing libraries as templates. The manipulation of maps and coordinate files was done with programs MAPMAN (*27*) and MOLEMAN (*28*), respectively.

The occupancies for NADP and the inhibitor molecules had to be adjusted to values less than 1.0 (*14*). Several values were selected for the refinement, and the behavior of the B factors was monitored. The occupancy was considered correct when the factors refined to values similar to the ones for atoms in close vicinity, which might lead to some underestimation of the actual occupancy. Further criteria were the behavior of R and R_{free} as well as the appearance of residual density in the F_o-F_c maps. Refinement of the inhibitor complexes converged with the R factors of less than 0.22 (R_{free} < 0.26) (Table 2). The coordinates have been deposited in the Protein Data Bank of Brookhaven (PDB), access codes 1dia, 1dib, and 1dig.

Site-Directed Mutagenesis. All mutations were performed using in vitro overlap-extension PCR with Vent DNA polymerase as described by the manufacturer (New England Biolabs). Amplification of DNA fragments using the first two sets of primers was performed in 10 mM KCl, 20 mM Tris-HCl (pH 8.8 at 25 °C), 10 mM $(NH_4)_2SO_4$, 3 mM $MgSO_4$, 0.1% Triton-X100, and 0.1 mg/mL BSA, using 10 ng of plasmid DNA, 125 μmol of each dNTP, 50 pmol of each primer, and 1 unit of Vent polymerase in a final volume of 50 μL. The samples were overlaid with 50 μL of light mineral oil and subjected to 30 cycles of PCR: denaturation, 30 s at 94 °C; annealing, 30 s at 50 °C; and extension, 30 s at 72 °C using a Progene (Techne) PCR machine. The products of the first PCR reactions were analyzed by electrophoresis on 1.6% agarose gels, and the bands of appropriate size were excised and purified using Gene-Clean (BIO/CAN Scientific) according to the manufacturer's specifications. One microliter of each of the overlapping fragments was mixed and subjected to PCR using the external primers under the same conditions, except that the annealing cycle was at 55 °C.

Following mutagenesis, a fragment containing the introduced mutation was excised by appropriate restriction digest and was used to replace the corresponding fragment in the wild-type expression plasmid. The entire fragment was sequenced to confirm the integrity of each mutant.

Enzyme Expression and Purification. The expression plasmid pBKe-DC301 (His_6-tagged at the C-terminus)

encoding wild-type dehydrogenase/cyclohydrolase, as well as all site-directed mutants, was used to transform *E. coli* BL21(DE23). Enzyme expression was obtained by induction of log-phase cultures with 0.4 mM IPTG as described previously (*29*). The bacterial cultures were centrifuged at 10 000 rpm (Sorvall RC5C, GSA rotor) for 10 min, and the cell pellets (1.5 g) were frozen at −80 °C. Frozen cells were resuspended in 3 vol of sonication buffer (0.1 M potassium phosphate, pH 7.3, 35 mM β-mercaptoethanol, 1 mM benzamidine, and 1 mM PMSF) and disrupted by sonication using six 15-s intervals separated by 1 min cooling in ice. After the addition of glycerol to 20% v/v, the extract was centrifuged at 16500*g* (Sorvall ss-34 rotor) for 30 min. One-tenth volume of 10% protamine sulfate was added to the supernatant solution, which was stirred on ice for 30 min and then centrifuged again for 30 min.

The supernatant solution was adjusted to 0.3 M NaCl and 5 mM imidazole (pH 7.8). To 6.5 mL of this solution was added 2 mL of a 50% slurry of Ni-NTA resin that had been equilibrated with buffer A (0.1 M potassium phosphate, pH 7.8, 35 mM β-mercaptoethanol, 1 mM benzamidine, 1 mM PMSF, 5 mM imidazole, and 20% glycerol). After 1 h of gentle mixing of the solution on an orbital shaker, the slurry was packed into a column (0.8 × 4 cm) and washed with 10 column vol each of buffer A containing 10 mM imidazole and buffer A containing 15 mM imidazole. The enzyme was eluted (0.2 mL/min) with buffer A containing 25 mM imidazole. Fractions containing enzyme activity were detected using standard activity assay conditions. All purifications were monitored by SDS−PAGE on 10% polyacrylamide gels, and protein was measured by a Bradford assay using BSA as the standard.

Dehydrogenase Assay. The assay mixture contained 25 mM MOPS (pH 7.3), 2 mM potassium phosphate (pH 7.3), 36 mM β-mercaptoethanol, 2.5 mM formaldehyde, 200 μM THF, and 400 μM NADP for standard conditions. For kinetic characterization in which the concentration of one substrate was varied, assays were performed at 30 °C with 2.5 mL assay mixtures by withdrawing 0.5-mL aliquots and adding them to 0.5 mL of 0.36 M HCl at 0-, 10-, 20-, and 30-s intervals. After 10 min, methenyltetrahydrofolate was determined by absorbance at 350 nm. Initial rates were determined from plots of methenyl-THF versus time. In all cases, a maximum of 10% of the limiting substrate was converted to product. For routine assays under saturation with both substrates, the standard fixed point assay was used (*29*).

Cyclohydrolase Activity. Cyclohydrolase activity was determined at 30 °C by following the initial rates of loss of methenyltetrahydrofolate at 355 nm on a recording spectrophotometer for 20 s and correcting for the nonenzymatic conversion of methenyltetrahydrofolate to 10-formyltetrahydrofolate. Assay buffer contained 25 mM MOPS (pH 7.3), 2 mM potassium phosphate, and 36 mM β-mercaptoethanol.

RESULTS AND DISCUSSION

General Structural Features. DC molecules form dimers, and there is one such dimer in the asymmetric unit in the crystal. Despite reasonable inhibition constants, the inhibitors appeared to bind to the enzyme with less than full occupancy or are partially disordered. Most interestingly, they bound to only one molecule of the dimer (referred to as molecule A). NADP is present in both molecules, A and B. The protein itself shows no significant structural change when compared to the crystal structure of the native enzyme complexed only with NADP. A loop of 10 amino acids close to the inhibitor binding site in molecule A cannot be found in the electron density, as is also the case in the native DC301 structure. In molecule B, this loop is well-ordered due to contacts with symmetry-related molecules in the crystal. No conformational changes were observed for amino acid side chains directly involved in NADP or inhibitor binding. Cys147 is an exception, as it is observed in two alternative conformations for its $C_\beta-C_\gamma$ bond in the Ly249543 and Ly374571 structures.

Both NADP and especially the inhibitor molecules appear to have partial occupancies in the crystal structure, with values ranging from 0.25 to 0.40, thus implying only weak protein−inhibitor interaction. Despite their relatively weak electron density, the orientation could always clearly be seen (Figure 3). The active site clefts in the two monomers A and B are of different widths as shown in Figure 4. The inhibitors bind only to the molecule with the narrower cleft (molecule A). Since the enzyme and the inhibitors were cocrystallized, this differential binding may be due to the intrinsic asymmetry of the dimers in solution rather than to crystal packing forces. The asymmetry within the dimer exists not only in this crystal form. Recently, we have solved the structure of the native protein in a monoclinic space group (*20*) and found that the two molecules in the asymmetric unit also show different widths of their active site clefts.

Inhibitor and Cofactor Binding. The inhibitors (Figure 2) bind in a cleft situated between the N- and the C-terminal domains of DC301. The fragment of the inhibitor corresponding to the reactive part in methylene-THF is sandwiched between the nicotinamide ring of NADP and the side chain of Tyr52 and is in proximity to the Lys56 side chain (Figure 5). The position with respect to the NADP is always such that the nicotinamide reactive carbon C^4 lies underneath the atoms corresponding to N^5 or N^{10} of methylene-THF. Contacts with the protein are mainly through interaction with backbone oxygens and nitrogens, suggesting that the binding site is preformed and rigid. Side chains interacting with the inhibitor are Gln100, Tyr52, and Lys56 (all inhibitors) and Asp125 in the case of Ly345899 (Figure 5). The position of the NADP molecule changes only slightly, but the nicotinamide part of the cofactor bound to monomer A shows some disorder with an inhibitor present.

The only chemically active group in proximity to the reactive center of the methenyl-THF molecule (or its analogue) is the ϵ-amino group of Lys56. Tyr52 and Lys56 are part of the Tyr−X−X−X−Lys motif strictly conserved in dehydrogenases/cyclohydrolases of the SCAD family (Figure 6) and are therefore the most probable candidates for catalytic residues. In the complexes, Tyr52 participates only in hydrophobic stacking interaction with the inhibitor molecule and is unlikely to play a direct role in the enzymatic reaction. Nevertheless, the contacts provided by Tyr52 are important for correct positioning of the substrate. Tyr52 does not interact with the Lys56 side chain, in contrast to other dehydrogenases (*9*, *14*). In the 3α-20β-hydroxysteroid dehydrogenase, the active site lysine amino group might adjust the pK_a of the tyrosine OH group so that its proton can easily be transferred to the substrate (*9*, *30*). In the DC301 molecule,

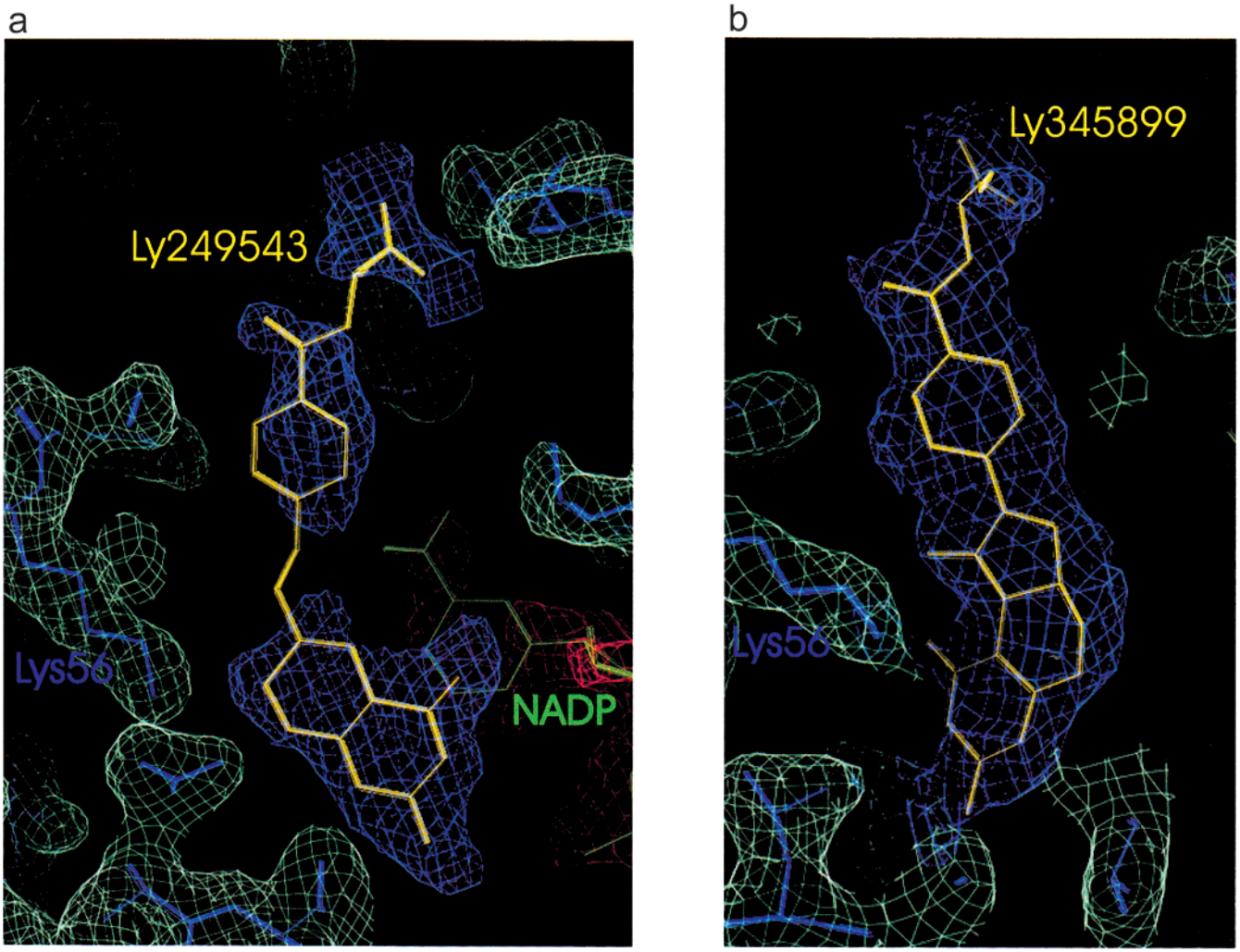

FIGURE 3: Electron density for inhibitors Ly249543 (a) and Ly345899 (b, σ weighted $2F_o-F_c$, contoured at 0.7 σ for the inhibitor and 1 σ for the protein and NADP) in similar orientation. Different orientation of the pteridine moiety in the two structures can clearly be seen. Figure produced in program O.

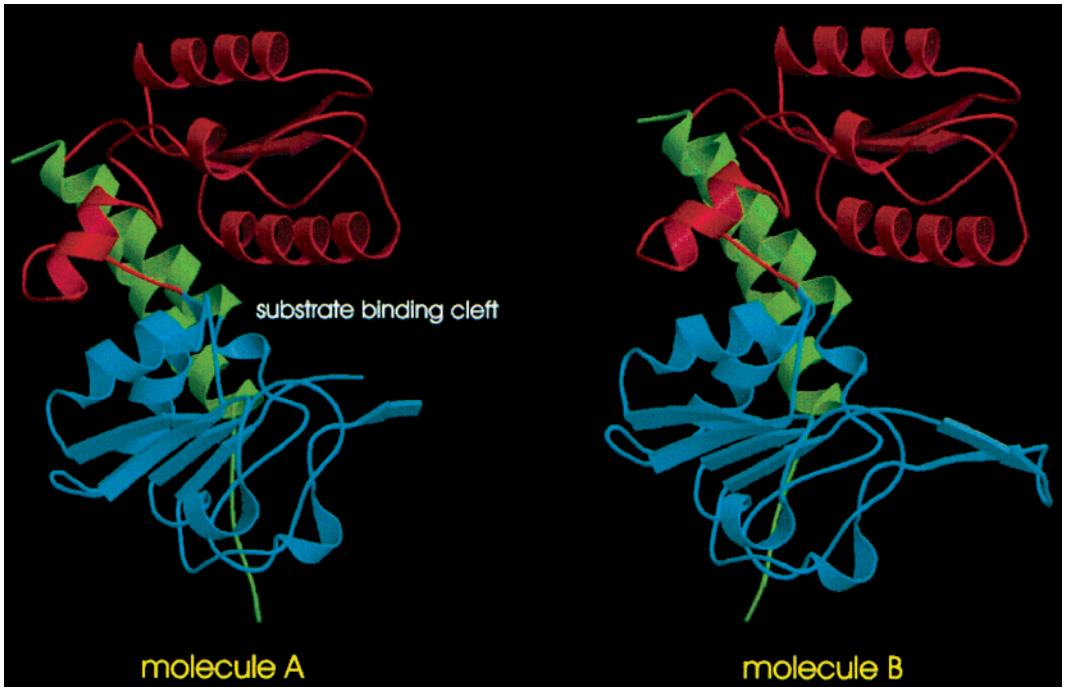

FIGURE 4: Ribbon representation [generated with MOLSCRIPT (*38*)] of the two molecules in the noncrystallographic dimer. Loop missing in molecule A is disordered. NADP binding domain is blue, catalytic domain is red, and hinge region is green. Inhibitors bound only to molecule A, with the narrower binding cleft.

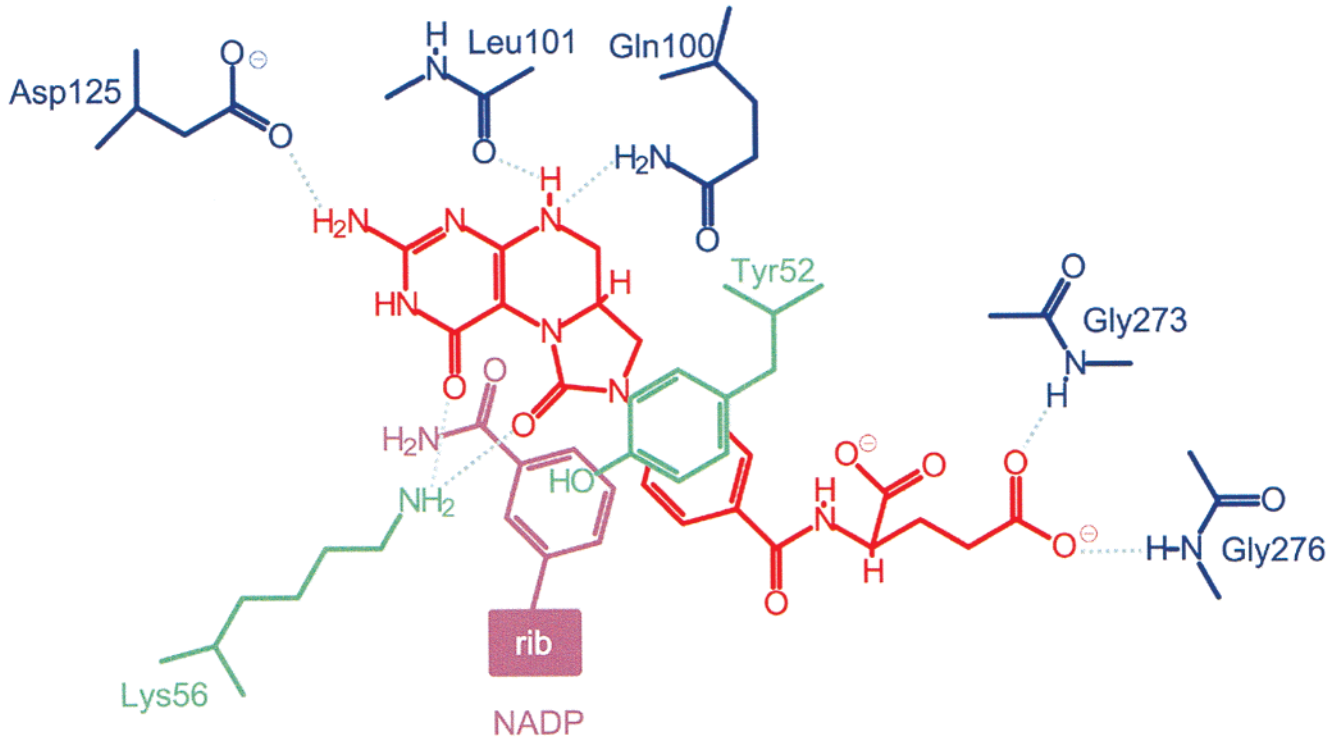

FIGURE 5: Environment of the bound Ly345899 inhibitor. Contacts between the protein and the substrate analogue are made mainly through backbone nitrogens and oxygens as well as hydrophobic stacking. Lys56 is positioned very well for chemical interaction.

```
DC_human_c    map-----------------------------------------------------AEILNGKEISAQIRARLKNQVTQLK   28
DC_rat_c      map-----------------------------------------------------AGILNGKVVSAQIRNRLKTQVTQMQ   28
DC_ecoli_c    ma------------------------------------------------------AKIIDGKTIAQQVRSEVAQKVQARI   27
DC_human_m    msalaarllqpahscslrlrpfhlaavrne--------------------------AVVISGRKLAQQIKQEVRQEVEEWV   55
DC_dros_m     matvmgptppgtgvmwpaiwrtsskaigirqsvqfefstrkisqkpqkevtisnmAQIIDGKAIAQEVRTQLAHELKGME   80
DC_mouse_m    masvsllsalavrllrpthgchprlqpfhlaavrne--------------------AVVISGRKLAQQIKQEVQQEVEEWV   61

DC_human_c    eqvpgfTPRLAILQVGNRDDSNLYINVKLKAAEEIGIKATHikLPRTTTESEVMKYITSLNEDSTVHGFLVQLPLdsens   108
DC_rat_c      eqvpgfTPGLAILQVGDRDDSNLYINVKLKAAQEIGIKATHikLPRTSTESEVLKYVISLNEDATVHGFIVQLPLdsens   108
DC_ecoli_c    aaglr-APGLAVVLVGSNPASQIYVASKRKACEEVGFVSRsydLPETTSEAELLELIDTLNADNTIDGILVQLPL--pag   104
DC_human_m    asgnk-RPHLSVILVGENPASHSYVLNKTRAAAVVGINSEtimKPASISEEELLNLINKLNNDDNVDGLLVQLPL--peh   132
DC_dros_m     aagyp-KPHLTAVIVGEDPASEKYVANKMVACREVGISSEtkrLPASTTQEELLQLIADLNKDPQVTGILVQLPV--peh   157
DC_mouse_m    asgnk-RPHLSVILVGDNPASHSYVLNKTRAAAEVGINSEtivKPASVSEEELLNSIRKLNNDENVDGLLVQLPL--peh   138

DC_human_c    inteevinaiapekdvdgltsiNAGRLARgdlndcFIPCTPKGCLELIKETGVPIAGRHAVVVGRSKIVGAPMHDLLLWN   188
DC_rat_c      inteavinaiapekdvdgltsiNAGKLARgdlkdcFIPCTPKGCLELIKETGVQIAGRHAVVVGRSKIVGAPMHDLLLWN   188
DC_ecoli_c    idnvkvlerihpdkdvdgfhpyNVGRLCQrapr--LRPCTPRGIVTLLERYNIDTFGLNAVVIGASNIVGRPMSMELLLA   182
DC_human_m    iderricnavspdkdvdgfhviNVGRMCLdqys--MLPATPWGVWEIIKRTGIPTLGKNVVVAGRSKNVGMPIAMLLHTD   210
DC_dros_m     inerticnavdvdkdvdgfnevNIGRTALdmea--NIPATPLGVKRLLEHMKIETLGRNAVVVGRSKNVSLPMAILLHAD   235
DC_mouse_m    iderkvcnavspdkdvdgfhviNVGRMCLdqys--MLPATPWGVWEIIKRTGIPTLGKNVVVAGRSKNVGMPIAMLLHTD   216

DC_human_c    ----------NATVTTCHSKTAHLDEEVNKGDILVVATGQPEMVKGEWIKPGAIVIDCGINYVPDDKkpngrKVVGDVAY   258
DC_rat_c      ----------NATVTTCHSKTADLDKEVNKGDILVVATGQPEMVKGEWIKPGAVVIDCGINYVPDDTkpngrKVVGDVAY   258
DC_ecoli_c    ----------GCTTTVTHRFTKNLRHHVENADLLIVAVGKPGFIPGDWIKEGAIVIDVGINRLENGK------VVGDVVF   246
DC_human_m    GAHERPGGDATVTISHRYTPKEQLKKHTILADIVISAAGIPNLITADMIKEGAAVIDVGINRVHDPVtakp-KLVGDVDF   289
DC_dros_m     GKYATKAMDATVTICHRYTPPKELARHCRQADIIVVAVGKPGLITKDMVKPGACVIDVGINRIKDEStgqf-KLVGDVDF   314
DC_mouse_m    GAHERPGGDATVTISHRYTPKEQLKKHTILADIVISAAGIPNLITADMIKEGAAVIDVGINRVQDPVtakp-KLVGDVDF   295

DC_human_c    DEAKERASFITPVPGGVGPMTVAMLMQSTVESAKRFLEkfkpgkwmiq-------                            306
DC_rat_c      DEAKEKASFITPVPGGVGPMTVAMLMQSTVESAQRFLKkfkpgkwtiq-------                            306
DC_ecoli_c    EDAAKRASYITPVPGGVGPMTVATLIENTLQACVEYHDpqde-------------                            288
DC_human_m    EGVRQKAGYITPVPGGVGPMTVAMLMKNTIIAAKKVLRleerevlkskelgvatn                            344
DC_dros_m     EEVRQVAGHITPVPGGVGPMTVAMLMHNTLKAARKQFDdrkss------------                            357
DC_mouse_m    EGVKKKAGYITPVPGGVGPMTVAMLMKNTIIAAKKVLRpeelevfkskqrgvatn                            350
```

FIGURE 6: Alignments of six DC sequences showing the conserved regions of these proteins. Sections interacting with NADP are blue, sections interacting with the inhibitors are yellow, and the active site residues are orange. Sequences shown are human, rat, and *E. coli* cytosolic DC (human_c, rat_c, ecoli_c) and human, drosophila, and mouse mitochondrial DC (human_m, dros_m, mouse_m). Alignment generated with MacawWin 2.0.0 (*39*).

Tyr52 forms H-bonding contacts only with Tyr240, located on the opposite side of the binding cleft at the beginning of the disordered loop region. This contact seems to be important for the correct positioning of the Tyr52 aromatic

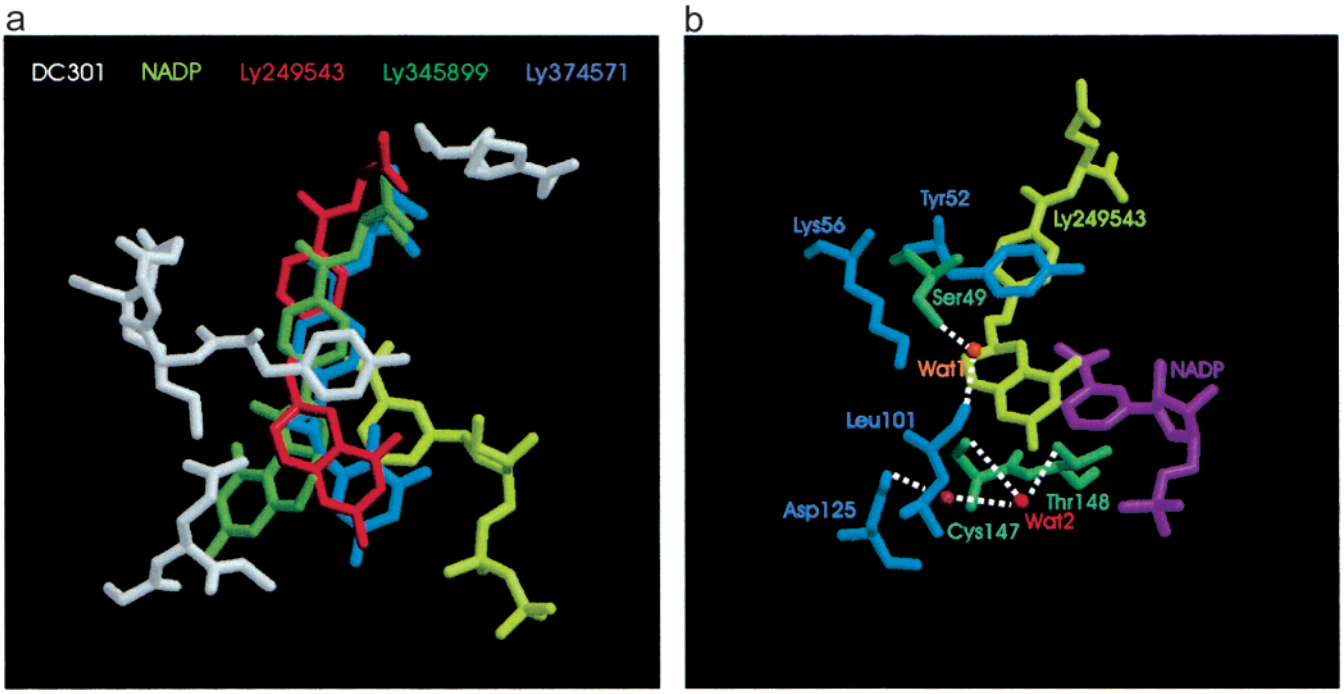

FIGURE 7: (a) Overlay of the three inhibitors as found in the crystal structures when the protein backbones are superimposed. All three inhibitors bind in the same region, with the same part of the molecule located close to the proposed active site. The pteridine moiety of Ly345899 is rotated by 180° relative to the other two inhibitors. Figure created with MOLSCRIPT (*38*). (b) Location of two water molecules near the catalytic site. Residues involved in binding these water molecules via direct H-bonds to their side chains are shown in green, and active site residues and residues binding the water molecules indirectly or with their backbone atoms are shown in blue.

Table 3: Inhibition Constants for the Inhibitors, Determined under Two Different Conditions

		K_i (μM)		
inhibitor	*M* (g/mol)	100% aq buffer	buffer + 4% DMSO	obsd in structure
Ly345899	471	0.018	0.029	yes
Ly249543	455		31.2	yes
Ly374571	431		0.003	yes
Ly289739	423	9.5	31.3	no

side chain. It is lost in molecule B, where the distance between the two OH group oxygen atoms is increased to 6.4 as compared to 3.8 Å in molecule A. The only strong H-bonding contacts formed by the side chain of Lys56 are with the Gln100 side chain (distance 2.6 Å).

In the Ly345899 complex, the orientation of the pteridine is flipped by 180° as compared to the two other inhibitors. This may be induced by the compound's additional carbonyl group, which allows for H-bonding contacts that are not possible with the other inhibitor molecules (Figure 7). Possible H-bonding partners in the other compounds (Ly249543 and Ly374571) are only provided by the nitrogens in the position corresponding to N^8 in THF, while the nitrogen N^5 is exchanged for an aliphatic carbon (Ly249543). In addition, the compound Ly374571 has a carbonyl group in position C^7 that does not exist in the natural substrate. The possibility for the pteridine moiety to assume two positions might also explain why the electron density for the more flexible inhibitors (such as Ly249543 and Ly374571) is weaker than for the very rigid Ly345899 molecule, even though kinetic data show that Ly374571 is the inhibitor with the lowest K_i (Table 3). Partial disorder of the nicotinamide ring of the NADP molecule bound to monomer A that occurs upon inhibitor binding has also been observed in other structures with bound NAD cofactor (*8*, *11*). In some cases, it is proposed that this effect is caused by free exchange between NAD and NADH present in the solvent. However, in the case of DC301, no NADPH was present in the crystallization medium, and the disorder suggests a slight movement of the nicotinamide moiety and its adjacent ribose group due to the interaction with the inhibitor molecule.

Kinetic Properties of Mutant Dehydrogenase/Cyclohydrolases. Tyrosine and lysine of the conserved Tyr−X−X−X−Lys motif have been proposed as catalytic residues for the dehydrogenase (*6*, *16*, *29*, *31*, *32*) and cyclohydrolase activities (*3*). Substitution by site-directed mutagenesis of Lys56 by Gln, Met, or Glu only moderately affected the dehydrogenase activity, while substitution by Ile, Ser, Thr, or Ala reduces it substantially, to 5−8% of wild-type activity (Table 4). Unexpectedly, the latter group of mutants exhibits reduced kinetic isotope effects when assayed with deuterated methylenetetrahydrofolate. All the above substitutions have a much more dramatic effect on the cyclohydrolase and render this function inactive (Table 5).

The K56R mutant does not follow the pattern just described. It retains approximately 1% of cyclohydrolase activity but, surprisingly, has the lowest residual dehydrogenase activity (0.8%) of any of the mutants. Also, it exhibits a normal kinetic isotope ratio.

The role of the Tyr52 residue in binding of the inhibitor rather than in catalysis is also consistent with kinetic investigation carried out on a Y52F mutant (Tables 4 and 5). The OH group of Tyr52 is not essential as a catalytic moiety for either activity since the Y52F mutant shows only minor reduction in dehydrogenase activity and no reduction in cyclohydrolase activity. The properties of Y52A and Y52S mutants are also consistent with this view; however, the effect on activity is more significant, and changes in the K_m values

Table 4: Kinetic Properties of Mutant DC, Showing the Effect on the Dehydrogenase Activity[a]

mutant	sp acty	K_m (μM) NADP	K_m (μM) methylene-THF	$^1H/^2H$
DC301 (wildtype)	**19**	**6.9 ± 1.1**	**4.0 ± 2.0**	**2.87**
K56R	0.2	5.9 ± 1.4	3.9 ± 1.1	2.62
K56E	**3.3**	**40.1 ± 1.0**	**5.7 ± 0.5**	**2.96**
K56S	0.4	21.7 ± 1.9	2.5	1.14
K56I	1.1	18.5 ± 3.7	3.2 ± 0.1	1.15
K56T	1.5	22.4 ± 3.4	1.6 ± 0.8	1.32
K56A	1.5	22.8 ± 2.9	2.0 ± 1.1	1.38
K56M	**6.1**	**106 ± 27**	**3.2 ± 0.4**	**2.70**
K56Q	**10.8**	**512 ± 84**	**2.1 ± 0.6**	**2.36**
S49A	17	≫500	ND	3.15
S49Q	5.6	10.3	3.7	2.15
Y52F	**9.6**	**46 ± 14**	**45.1 ± 8.1**	**ND**
Y52S	0.2	2.9 ± 0.3	3.2 ± 2.0	ND
Y52A	0.2	1.7 ± 0.4	4.5 ± 1.4	ND
C147Q	7.9	4.7	8.9	2.29
C147A, T148A	2.2	4.5	1.3	2.29
C147Q, S49Q	8.0	4.0	8.5	3.34

[a] Mutants with high residual activity are in boldface.

Table 5: Kinetic Properties of Mutant DC, Showing the Effect on the Cyclohydrolase Activity[a]

mutant	specific activity (units/mg)	K_m methylene-THF (μM)
DC 301 (wildtype)	**133**	**34 ± 19**
K56R	**1.6**	**14 ± 11**
K56E	ND	ND
K56S	ND	ND
K56I	ND	ND
K56T	ND	ND
K56A	ND	ND
K56M	ND	ND
K56Q	ND	ND
S49A	128	52 ± 9
S49Q	25	32
Y52F	**160**	**48 ± 16**
Y52S	39	162 ± 5
Y52A	47	122 ± 25
C147Q	18	236
C147A, T148A	146	56
C147Q, S49Q	6.7	ND

[a] Mutants with high residual activity are in boldface.

for the substrates are more pronounced. The slightly elevated kinetic isotope ratios for the Y52 mutants suggest that the alignment of the bound substrates has been altered in these enzymes.

The cyclohydrolase activity, in the forward direction, uses a water molecule to hydrolyze the methenyl intermediate. Residues Ser49 and Cys147 interact with water molecules bound in the vicinity of the active site, termed Wat1 and Wat2, respectively. These residues were tested for their effect on cyclohydrolase activity. Wat1 makes H-bonds not only to Ser49 but also to the backbone oxygen atom of Leu101. The S49A mutant exhibits normal cyclohydrolase activity, while the S49Q mutant has only 19% of wild-type activity. Serine to alanine replacement creates a larger void and may not prevent the binding of a water molecule. Introduction of a larger Gln was designed to eliminate this water binding site. A significant residual cyclohydrolase activity of this S49Q precludes the notion that this water molecule is utilized solely in this enzymatic mechanism.

The second bound water molecule interacts with Cys147 and Thr148. Cys147 is strictly conserved in all cytosolic enzymes of this type, and Thr148 is strictly conserved throughout the sequences of both cytosolic and mitochondrial enzymes. The cyclohydrolase activity of the C147A/T148A double mutant is unaffected, downplaying the role of Wat2 in the reaction. The C147Q mutant, which is expected to block proper binding of the water molecule, still retains 14% activity, suggesting that this specific water molecule is also not solely involved in the cyclohydrolase reaction.

Implications for the Reaction Mechanism. The structures of three inhibitor complexes depicted quite clearly the interactions between the protein and its substrate. They allowed us to propose a novel assignment of residues involved in catalysis and the details of the reaction mechanism (Figure 8).

On the basis of the conservation pattern and the location in the enzyme, we proposed previously that Tyr52 and Lys56 constitute the active site for the cyclohydrolase function (*3*). In the crystal structures of the complexes, Tyr52 stacks with the aromatic rings of the inhibitors and is unlikely to take part in catalysis. Indeed, replacement of this residue by a phenylalanine, which lacks the OH group necessary for chemical action, had practically no effect on the enzymatic activity.

Mutations of Lys56 completely inactivated the cyclohydrolase and significantly reduced the dehydrogenase activity in a manner dependent on the type of substitution. We therefore propose that Lys56 plays a role in both reactions and changes its function in the course of channeling the substrate from dehydrogenase to cyclohydrolase activity. In the dehydrogenase step as depicted in Figure 8, the Lys56 amino group increases the electron density in the tetrahydropteridine moiety, thereby assisting the abstraction of a hydride from the methylene group by the nicotinamide moiety of NADP. In the cyclohydrolase reaction, Lys56 is proposed to play a role in proton transfer, assisting the conversion of the hydroxymethyl intermediate to 10-formyltetrahydrofolate.

In either of the proposed functions, the lysine ϵ-amino group must be in the neutral state, as NH_2. The normal pK_a for the lysine side chain is around 10. Thus, an environment must exist that favors the nonprotonated state for this residue at physiological pH. In the crystal structure, Lys56 is embedded in a strongly hydrophobic environment that favors the nonprotonated form. Of the 11 residues constituting the close environment of Lys56 (Figure 9), eight are hydrophobic (of the type Leu, Ile, Val, or Met, plus Tyr52). In six DC protein sequences, four of those are strictly conserved (Val280, Leu283, Tyr52, and Leu38), and the others are highly conserved (Met284, Ile40, Ile53, and Leu98). This strongly hydrophobic environment might be of extreme importance for the reverse cyclohydrolase reaction, in which an intermediate sensitive to hydrolysis is being formed. There are known cases in which a lysine side chain shows an unusually low pK_a and therefore acts as a general base during catalysis. In RTEM β-lactamase from *E. coli*, the active site lysine was found to have strong H-bonding contacts with a nearby serine and a glutamine (*33*), as is the case in DC301. In addition, proximity to another lysine disfavors protonation of the catalytically active lysine (*34*), effectively lowering its pK_a down to values between 6 and 7. This effect was

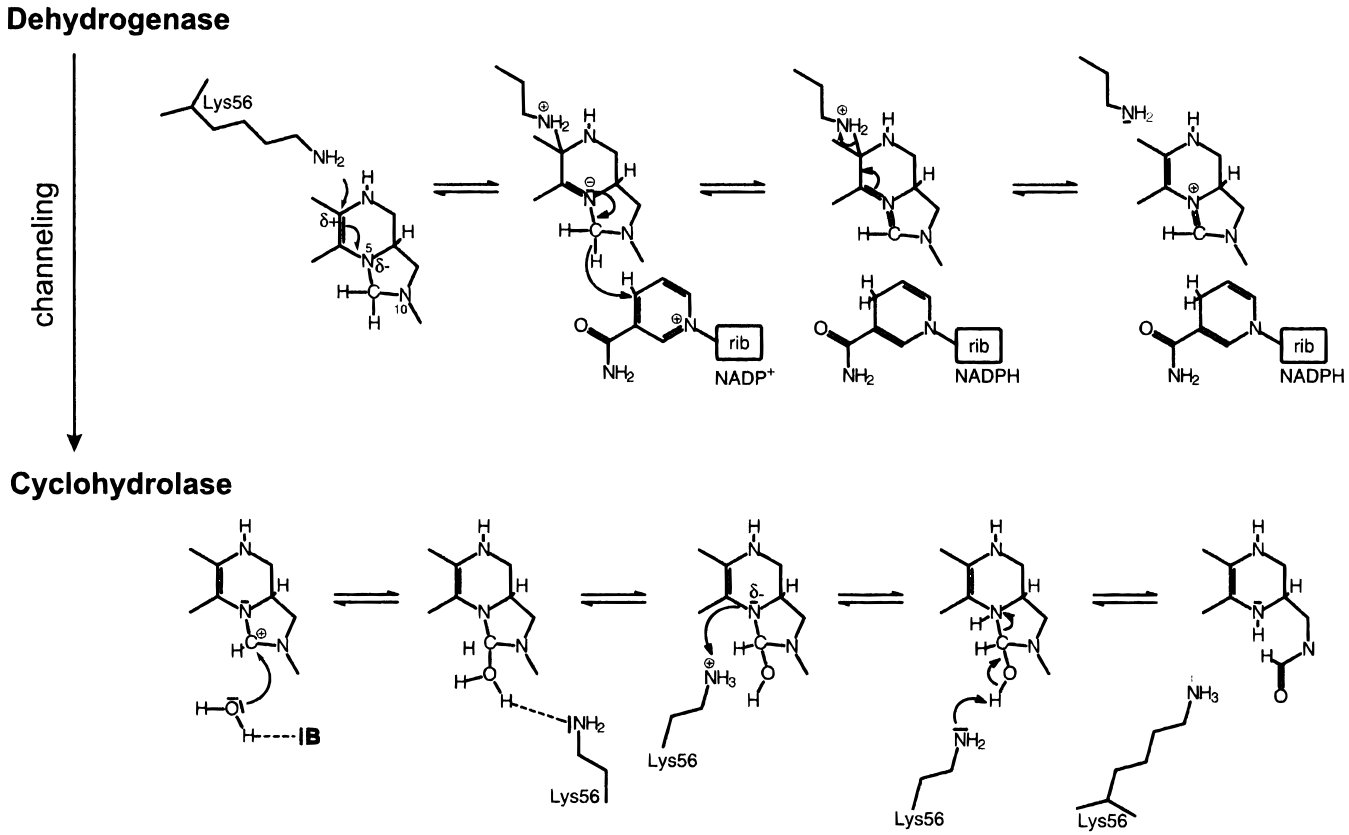

FIGURE 8: Proposed reaction mechanism for DC301. Lys56 is proposed to play a key role in both reaction steps and to change its function from a Lewis base in the dehydrogenase step to an actual proton acceptor/donor in the cyclohydrolase step. This reaction scheme involves a rotation of the pteridine fragment by 180°. The water molecule in the cyclohydrolase step might come from the solvent or be held nearby by the base "B", which could be Ser49, Cys147, or Thr148. Figure drawn withChemWindows 5.0/CorelDraw 7.

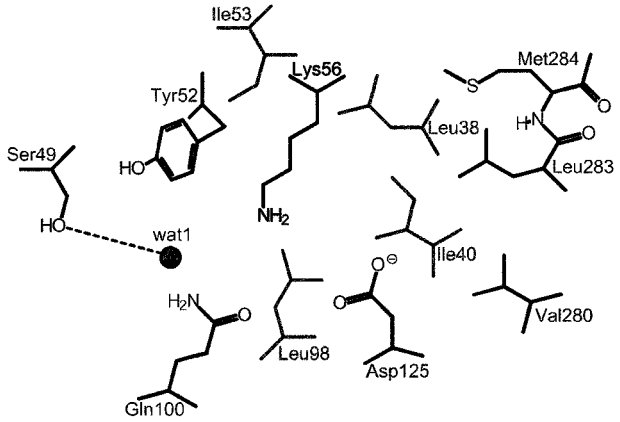

FIGURE 9: Environment of the lysine 56 side chain. Most of the residues surrounding this amino acid are hydrophobic and would therefore destabilize the protonated form of Lys56. All of these residues are highly conserved.

also detected earlier in an investigation of mellitin (*35*) and ribulose-1,5-bisphosphate carboxylase (*36*). In these cases, the ionization constants for the active site lysine, located in a positively charged environment, were considerably shifted. Lysine can also replace the histidine of a catalytic triad, which then acts as a general base (*37*).

For Lys56 to play both roles, it would require a change of orientation of the substrate within the active site cleft. This movement would thus represent the transfer between two catalytic sites (i.e., channeling) and might be a step at which about half the intermediate is known to be released from the site. In DC301, the rather wide binding cleft and the mobility of protein domains could allow for such movements. As inferred from the structure of complexes, the interactions of the substrate in both possible orientations with the protein and NADP would be very similar, suggesting small energy differences between the two orientations. Molecular dynamics calculations on the methylenetetrahydrofolate dehydrogenase/cyclohydrolase from *E. coli* (*4*) indicated that the pteridine moiety of the substrate might turn between the two reaction steps. Ly345899, with an additional contact between the N^8 atom of the pteridine ring analogue and the Asp125 side chain, best represents the binding of methenyl-THF or N^{10}-formyl-THF (the substrate for the reverse cyclohydrolase reaction), while the two other inhibitors correspond to the methylene-THF substrate. The way the substrate binds to the protein could be guided by its chemical properties. The carbonyl group of N^{10}-formyl-THF is an excellent H-bonding partner for a lysine side chain, while the weakly polarized methylene-THF is more likely to bind with the less negatively charged side of the pteridine moiety next to the unprotonated lysine.

Dehydrogenase. Mutations of Lys56 to amino acid side chains capable of providing a free electron pair (K56M, K56Q, and K56E) exhibit significantly higher dehydrogenase activity than those of similar size (K56I and K56T) that cannot. According to the findings in the crystal structure as well as the kinetic investigation of the mutants, Lys56 would have the role of a nucleophile in the dehydrogenase step. As an electron donor, it could carry out a nucleophilic attack on the aromatic system in the pteridine moiety and, by generating an excess of electrons in the substrate molecule, assist

the release of a hydride to the NADP cofactor (Figure 8). The polarization (or adduct formation) and the hydride transfer steps are most likely to be concerted. This hydride transfer is normally rate-limiting, exhibiting a deuterium kinetic isotope effect of about 2.9. In mutants lacking the Lewis base side chain at position 56, the kinetic isotope effect is reduced (Table 4) consistent with lower efficiency of an earlier step, such as activation of the tetrahydropteridine ring.

However, whether the effect of the lysine's attack is only polarization or the formation of an actual adduct remains unclear. The only possible target for adduct formation is C^9, which carries a positive partial charge due to its position between two electronegative nitrogen atoms. The inhibitors Ly249543 and Ly289739 have correct orientation for Lys56 to perform this nucleophilic attack, while the pteridine analogue part of Ly345899 is already rotated into a position suitable for the cyclohydrolase reaction. With the dehydrogenase reaction completed, we propose that the function of Lys56 becomes the stabilization of the positively charged methenyl intermediate.

Cyclohydrolase. All mutations at position 56, except K56R, abolished cyclohydrolase activity. The results indicate that the amino acid in position 56 has to be capable of taking up a proton. The residues that can provide a free electron pair and hence negative partial charge (K56Q, K56M, and K56E) are still active as a dehydrogenase but are not capable of actually taking up a proton and therefore lost the cyclohydrolase activity.

A different behavior of active site Lys56 toward the methylene-THF substrate and in the cyclohydrolase reaction might simply be induced by the reactants themselves. During the cyclohydrolase reaction, the unstable reaction intermediate strongly offers a proton that can be taken up by Lys56. After catalysis is completed and the products are released, this lysine would lose the proton to the surrounding solvent at its low pK_a. However, two bases are needed for the reaction to occur: one to activate the water molecule (Figure 8), which then attacks the methenyl intermediate, and the second, Lys56, to abstract a proton and induce the formation of 10-formyltetrahydrofolate by reprotonation of N^5.

As the substrate binding pocket has mostly hydrophobic character, with only a few solvent molecules present, the attacking water molecule must reside in proximity to the substrate, being at the same time activated. Two water molecules are situated near the substrate binding site (Figure 7b). Wat1 is H-bonded to Ser49, a residue that is part of the "top" of the cleft and strictly conserved in this protein class. Wat2 participates in an H-bonding network with the side chains of Cys147, Thr148, and Asp125 and the backbone carbonyl of Leu101. Although in favorable positions, none of these waters could be proven to participate in the cyclohydrolase reaction, and thus the roles of conserved Ser49, Cys147, and Thr148 are uncertain.

CONCLUSIONS

These experiments have provided insight into the binding of folate substrates to the catalytic cleft of the DC bifunctional enzyme. Using these structures in combination with the kinetic properties of mutant proteins, we have proposed a binding/orientation role for Tyr52 in substrate binding and a catalytic role for Lys56 in both the dehydrogenase and the cyclohydrolase reactions. Lys56 appears to have a pK_a that is considerably lower than normal and could be a target for amino- specific agents. For example, reactive folate analogues could be designed to be very efficient covalent inhibitors of this bifunctional site.

ACKNOWLEDGMENT

We thank Yunge Li for her help with the crystallization and the crystal handling and Marc Allaire for collecting data for the Ly345899 complex. We thank the Sheldon Biotechnology Center, McGill University, for synthesis of PCR primers and DNA sequencing.

SUPPORTING INFORMATION AVAILABLE

Synthesis of the inhibitors (3 pages). This material is available free of charge via the Internet at http://pubs.acs.org.

REFERENCES

1. Green, J. M., MacKenzie, R. E., and Matthews, R. G. (1988) *Biochemistry 27*, 8014−8022.
2. Pawelek, P. D., and MacKenzie, R. E. (1998) *Biochemistry 37*, 1109−1115.
3. Allaire, M., Li, Y., MacKenzie, R. E., and Cygler, M. (1998) *Structure 6*, 173−182.
4. Shen, B. W., Dyer, D. H., Huang, J.-H., D'Ari, L., Rabinowitz, J., and Stoddard, B. L. (1999) *Protein Sci. 8*, 1342−1349.
5. Rossmann, M. G., and Olsen, K. W. (1974) *Nature 250*, 194−199.
6. Jornvall, H., Persson, B., Krook, M., Atrian, S., Gonzalez-Duarte, R., Jeffery, J., and Ghosh, D. (1995) *Biochemistry 34*, 6003−6013.
7. Ghosh, D., Wawrzak, Z., Weeks, C. M., Duax, W. L., and Erman, M. (1994) *Structure 2*, 629−640.
8. Baldock, C., Rafferty, J. B., Stuitje, A. R., Slabas, A. R., and Rice, D. W. (1998) *J. Mol. Biol. 284*, 1529−1546.
9. Ghosh, D., Weeks, C. M., Grochulsky, P., Duax, W. L., Erman, M., Rimsay, R. A., and Orr, J. C. (1991) *Proc. Natl. Acad. Sci. U.S.A. 88*, 10064−10068.
10. Liu, Z.-J., Sun, Y.-J., Rose, J., Chung, Y.-J., Hsiao, C.-D., Chang, W.-R., Kuo, I., Perozich, J., Lindahl, R., Hempel, J., and Wang, B.-C. (1997) *Nat. Struct. Biol. 4*, 317−326.
11. Rafferty, J. B., Simon, J. W., Baldock, C., Artymiuk, P. J., Baker, P. J., Stuitje, A. R., Slabas, A. R., and Rice, D. W. (1995) *Structure 3*, 927−938.
12. Varughese, K. I., Skinner, M. M., Whiteley, J. M., Matthews, D. A., and Xuong, N. H. (1992) *Proc. Natl. Acad. Sci. U.S.A. 89*, 6080−6084.
13. Auerbach, G., Ostendorp, R., Prade, L., Korndorfer, I., Dams, T., Huber, R., and Jaenicke, R. (1998) *Structure 6*, 769−781.
14. Breton, R., Housset, D., Mazza, C., and Fontecilla-Camps, J. C. (1996) *Structure 4*, 905−915.
15. Hurley, J. H., Dean, A. M., Koshland, D. E. J., and Stroud, R. M. (1991) *Biochemistry 30*, 8671−8678.
16. Pelletier, J. N., and MacKenzie, R. E. (1995) *Biochemistry 34*, 12673−12680.
17. Chen, V. J., Bewley, J. R., Andis, S. L., Schulz, R. M., Iversen, P. W., Shih, C., Mendelsohn, L. G., Seitz, D. E., and Tonkinson, J. L. (1998) *Br. J. Cancer 78*, 27−34.
18. Shih, C., Chen, V. J., Gossett, L. S., Gates, S. B., McKellar, W. C., Habeck, L. L., Shackelford, K. A., Mendelsohn, L. G., Soose, D. J., Patel, V. F., Andis, S. L., Bewley, J. R., Rayl, E. A., Moroson, B. A., Beardsley, G. P., Kohler, W., Ratnam, M., and Schultz, R. M. (1997) *Cancer Res. 57*, 1116−1123.
19. Tonkinson, J. L., Habeck, L. L., Toth, J. E., Mendelsohn, L. G., Bewley, J. R., Shackelford, K. A., Gates, S. B., Ray, J., and Chen, V. J. (1998) *J. Pharmacol. Exp. Ther. 287*, 315−321.
20. Allaire, M., Li, Y., Meija, N. R., Pelletier, J. N., MacKenzie, R. E., and Cygler, M. (1996) *Proteins 26*, 479−480.

21. Taylor, E. C., Harrington, P. J., Fletcher, S. R., Beardsley, G. P., and Moran, R. G. (1985) *J. Med. Chem. 28*, 914−921.
22. Otwinowsky, Z., and Minor, W. (1997) *Methods Enzymol. 276*, 307−326.
23. Bailey, S. (1994) *Acta Crystallogr. D50*, 760−763.
24. Brunger, A. T., Kuriyan, J., and Karplus, M. (1987) *Science 235*, 458−460.
25. Brunger, A. T., Krukowski, A., and Erickson, J. (1992) *Nature 355*, 472−474.
26. Jones, T. A., Zou, J. Y., Cowan, S., and Kjeldgaard, M. (1991) *Acta Crystallogr. A47*, 110−119.
27. Kleywegt, G. J., and Jones, T. A. (1996) *Acta Crystallogr. D55*, 941−944.
28. Kleywegt, G. J. (1997) *J. Mol. Biol. 273*, 371−376.
29. Hum, D. W., and MacKenzie, R. E. (1991) *Protein Eng. 4*, 493−500.
30. Benach, J., Atrian, S., Gonzales-Duarte, R., and Ladenstein, R. (1998) *J. Mol. Biol. 282*, 383−399.
31. Chen, Z., Jiang, J. C., Lin, Z.-G., Lee, W. R., Baker, M. E., and Chang, S. H. (1993) *Biochemistry 32*, 3342−3346.
32. Ribas de Pouplana, L., and Fothergill-Gilmore, L. A. (1994) *Biochemistry 33*, 7047−7055.
33. Strynadka, N. C. J., Adachi, H., Jensen, S. E., Johns, K., Sielecki, A., Betzel, C., Sutoh, K., and James, M. N. G. (1992) *Nature 359*, 700−705.
34. Oefner, C., D'Arcy, A., Daly, J. J., Gubernator, K., Charnas, R. L., Heinze, I., Hubschwerlen, C., and Winkler, F. K. (1990) *Nature 343*, 284−288.
35. Quay, S. C., and Tronson, L. P. (1983) *Biochemistry 22*, 700−707.
36. Lu, G. G., Lindqvist, Y., and Schneider, G. (1992) *Proteins 12*, 117−127.
37. Monnaie, D., Dubus, A., Cooke, D., Marchand-Brynaert, J., Normark, S., and Frere, J.-M. (1994) *Biochemistry 33*, 5193−5201.
38. Kraulis, P. J. (1991) *J. Appl. Crystallogr. 24*, 946−950.
39. Schuler, G., Altschul, S. F., and Lipman, D. J. (1991) *Proteins: Struct., Funct., Genet. 9*, 180−190.

BI992734Y